Univerzita Karlova

1. lékařská fakulta

Autoreferát disertační práce

UNIVERZITA KARLOVA
1. lékařská fakulta

Neuroprotektivní účinky nových anorektických analogů peptidu uvolňujícího prolaktin (PrRP) v modelech neurodegenerace *in vitro* a *in vivo*

Neuroprotective effects of novel anorexigenic analogs of prolactin-releasing peptide (PrRP) in models of neurodegeneration *in vitro* and *in vivo*

Ing. Anna Mengr (roz. Zmeškalová)

Praha, 2022

Doktorské studijní programy v biomedicíně

Univerzita Karlova a Akademie věd České republiky

Studijní program: Biochemie a patobiochemie

Studijní obor: Biochemie a patobiochemie

Předseda oborové rady: Prof. MUDr. Zdeněk Kleibl, PhD.

Školicí pracoviště: Ústav organické chemie a biochemie Akademie věd České repuliky, v.v.i.

Školitelka: RNDr. Lenka Maletínská, CSc.

Disertační práce bude nejméně pět pracovních dnů před konáním obhajoby zveřejněna k nahlížení veřejnosti v tištěné podobě na Oddělení pro vědeckou činnost a zahraniční styky Děkanátu 1. lékařské fakulty.

ABSTRAKT

Alzheimerova choroba (AD) je progresivní mozková porucha charakterizovaná extracelulárními beta amyloidními (Aβ) plaky, intracelulárními neurofibrilárními klubky tvořenými hyperfosforylovaným proteinem Tau a zánětem. Vzhledem k tomu, že obezita a diabetes mellitus 2. typu (T2DM) byly stanoveny jako rizikové faktory pro rozvoj neurologických poruch, anorexigenní a antidiabetické peptidy, jako je peptid uvolňující prolaktin (PrRP), se zdají být potenciálními neuroprotektivními látkami.

V první části práce byly studovány molekulární mechanismy účinku přirozeného PrRP31 a jeho lipidovaného analogu palm^{11}-PrRP31 v buněčné linii lidského neuroblastomu SH-SY5Y. Oba peptidy významně aktivovaly signální dráhy typické pro insulin podporující přežití a růst buněk. Kromě toho PrRP31 a palm^{11}-PrRP31 zvýšily životaschopnost buněk a potlačily apoptózu v buňkách SH-SY5Y stresovaných methylglyoxalem.

Druhá část práce byla zaměřena na neuroprotektivní a protizánětlivé účinky v mozku APP/PS1 myší, modelu Aβ patologie, po subkutánním podávání palm^{11}-PrRP31 po dobu 2 měsíců. Palm^{11}-PrRP31 signifikantně snížil množství Aβ plaků a mikrogliózu v hipokampech, kortexech a mozečku. Kromě toho palm^{11}-PrRP31 zvýšil synaptogenezi a zmírnil centrální zánět a apoptózu v hipokampu myší APP/PS1.

Ve třetí části práce byl sledován potenciální vztah mezi insulinovou rezistencí a AD v mozcích a periferii myší APP/PS1 krmených dietou s vysokým obsahem tuků (HFD), modelu spojující obezitu a patologii podobnou AD. HFD zhoršila Aβ patologii v hipokampech a významně ovlivnila jak centrální, tak periferní zánět. Kromě toho se u myší na HFD vyvinula výrazná periferní inzulínová rezistence vedoucí k centrální inzulínové rezistenci. Studie odhalila škodlivý vliv zánětu souvisejícího s obezitou a prediabetem na rozvoj Aβ patologie a zánětu v mozku a potvrdila periferní a centrální zánět a inzulínovou rezistenci jako potenciální mediátory mozkové dysfunkce u AD.

Závěrem, moje práce prokazuje příznivý účinek PrRP na patologii podobnou AD, což naznačuje, že palm^{11}-PrRP31 může být slibnou látkou pro léčbu AD.

KLÍČOVÁ SLOVA

Alzheimerova choroba, obezita, zánět, centrální zánět, APP/PS1 myši, Aβ plaky, Tau, inzulinová rezistence, buňky SH-SY5Y, peptid uvolňující prolAktin

ABSTRACT

Alzheimer´s disease (AD) is a progressive brain disorder characterized by extracellular beta amyloid (Aβ) plaques, intracellular neurofibrillary tangles formed by hyperphosphorylated Tau protein and neuroinflammation. Since obesity and type 2 diabetes mellitus (T2DM) have been established as risk factors for the development of neurological disorders, anorexigenic and antidiabetic peptides, such as prolactin-releasing peptide (PrRP) seem to be potential neuroprotective agents.

In the first part of the study, the molecular mechanisms of action of natural PrRP31 and its lipidized analog palm^{11}-PrRP31 was studied in the human neuroblastoma cell line SH-SY5Y. Both compounds significantly activated the signaling pathways typical for insulin promoting cell survival and growth. Moreover, PrRP31 and palm^{11}-PrRP31 increased cell viability and suppressed apoptosis in methylglyoxal-stressed SH-SY5Y cells.

The second part of the thesis was focused on the neuroprotective and anti-inflammatory effects of 2-month-long subcutaneous administration of palm^{11}-PrRP31 in the brains of APP/PS1 mice, model of Aβ pathology. Palm^{11}-PrRP31 significantly reduced the Aβ plaque load and microgliosis in the hippocampi, cortices, and cerebella. Furthermore, palm^{11}-PrRP31 increased the synaptogenesis and attenuated neuroinflammation and apoptosis in the hippocampus of APP/PS1 mice.

In the third part of the thesis, a potential relationship between insulin resistance and AD was followed in the brains and periphery of APP/PS1 mice fed with high-fat diet (HFD), the model connecting obesity and AD-like pathology. HFD worsened the Aβ pathology in hippocampi and significantly affected both central and peripheral inflammation. Furthermore, mice on HFD developed substantial peripheral insulin resistance leading to central insulin resistance. The study revealed a deleterious effect of obesity-related inflammation and pre-diabetes on the development of Aβ pathology and neuroinflammation and confirmed peripheral and central inflammation and insulin resistance as potential mediators of brain dysfunction in AD.

In conclusion, my thesis proves beneficial effect of PrRP in the AD-like pathology, suggesting palm^{11}-PrRP31 as a promising agent for the treatment of AD.

KEY WORDS:

Alzheimer´s disease, obesity, inflammation, neuroinflammation, APP/PS1 mice, Aβ plaques, Tau, insulin resistance, SH-SY5Y cells, prolactin-releasing peptide

CONTENT

1. INTRODUCTION

Alzheimer's disease (AD), an age-associated neurological disorder affecting regions of the brain that control memory and cognitive functions is the most common type of dementia globally, accounting for 60 - 80% of all dementia cases [1]. Two major pathological hallmarks of AD are extracellular senile plaques formed by amyloid-β (Aβ) peptide and intracellular neurofibrillary tangles (NFTs) formed by hyperphosphorylated Tau protein. In addition, AD is characterized by neuroinflammation, extensive loss of synapses, loss of neurons in vulnerable regions and subsequent structural changes in the brain, including hippocampal volume loss, brain atrophy and disturbed insulin and glucose metabolism in the brain [2].

Neuroinflammation, one of the main indicators of AD progression, is characterized by reactive astrocytes and microglia, which are typically found in excess around neurons and Aβ plaques and are therefore thought to be a result of ongoing deposition of Aβ [3]. Activated astrocytes and microglia produce proinflammatory molecules, such as cytokines that are increased in AD brain tissue and are thought to play a role in neuronal degeneration and in establishing chronic inflammation [4]. Astrocytes are further involved in the clearance of soluble Aβ peptide from the brain parenchyma by glymphatic paravenous drainage [5]. This pathway is believed to depend on the astrocytic water channel aquaporin-4 (AQ4), since its deletion resulted in a strong decrease in Aβ peptide clearance.

Loss of synapses, which is associated with the disruption of neuronal plasticity, is implicated in early AD pathology and may be robust even before overt neurodegeneration and brain atrophy [6]. However, many direct and some indirect effect, such as inflammation and insulin resistance (IR), have been suggested to play an important role in pathological synaptic dysfunction [7].

Most of the research in the AD field has focused on the earliest affected and most vulnerable brain areas damaged during AD, hippocampus, entorhinal cortex and perirhinal cortex, as they are considered the primary regions responsible for the formation of memories and spatial cognition [8]. However, recent studies have also demonstrated that Aβ deposits are found within the molecular, granular and Purkinje cell layers of the cerebellar cortex. The number of Aβ deposits has been shown to increase with disease progression in the cerebellar cortex in both patients and mouse models of AD. In contrast, NFTs are mostly absent in the cerebellum [9].

Insulin was detected in various brain areas under physiological conditions, especially in the cortex, hippocampus, and hypothalamus, and its signaling is essential for the proper functioning of the brain [10]. Hyperinsulinemia leading to IR is a pathological condition, in which target tissues are not physiologically responsive to insulin [11]. The central IR leads to the impairment of insulin signaling in the brain, which induces the hyperphosphorylation of Tau protein and formation of Aβ oligomers by the multiple mechanisms, this points to a link between IR and AD [10b].

Obesity is defined as a medical condition at which excess body fat has accumulated to the extent that it may have an adverse effect on health. It is further associated with other metabolic disturbances, such as hyperglycemia, hyperinsulinemia, IR and peripheral inflammation; all of them are related to the development of AD and are therefore widely accepted as risk factors of AD [10b]. However, ageing is number one AD risk [12].

In rodents, high-fat diet (HFD)-induced IR exhibited a cognitive decline with impaired insulin regulation, increased inflammation, mitochondrial dysfunction, increased oxidative stress, and apoptosis in the brain [10b, 13]. These results suggest that chronic peripheral IR can induce brain IR and brain dysfunction. Due to the same patterns of disturbance in insulin signaling and IR in the brain and periphery, AD is sometimes called Type 3 diabetes [14].

Often used *in vitro* models for neurodegenerative disorders are SH-SY5Y cells and primary neuronal culture. SH-SY5Y is a subcloned cell line derived from human neuroblastoma cell line, isolated from a metastatic bone tumor that can be differentiated from a neuroblast-like state into mature human neurons. Primary neuronal culture refers to *in vitro* maintenance of living neurons that have been extracted from animal nervous system tissue such as brain or spinal cord.

The action of neurotoxic agents such as methylglyoxal (MG) on neuroblastoma cell lines that causes an increase in oxygen radicals and subsequently reduces cell viability is one approach to induce neurodegeneration *in vitro* [15]. Moreover, MG increases the levels of pro-apoptotic proteins that are essential for the onset of apoptosis and is associated with an extended synapse disorder, which is an early sign of AD [16].

The animal models are an important and fundamental part of medical research. Several rodent models were designed to investigate the pathological processes leading to development of AD, obesity, or IR. In recent years, many models combining all of the above-mentioned diseases were used to examine the effect of obesity and related T2DM on the development of neurological disorders, such as dementia or AD.

APP_{swe}/$PSEN1_{dE9}$ (APP/PS1) mice, a transgenic mouse model of amyloidosis, combine the Swedish mutation in APP (K670N/M671L) (SWE) and mutation in presenilin 1 ($PSEN1_{dE9}$). APP/PS1 mice are characterized by a pronounced increase in Aβ deposits in the hippocampus and cortex, compared to their littermates without mutations, impaired score in behavioral experiments and increased brain oxidative stress markers [17].

Rodents with diet induced obesity (DIO) are considered models of the most common human obesity, which is associated with the consumption of high energetic diet, mostly HFD [18]. HFD feeding increases amount of adipose tissue, which consequently leads to hyperleptinemia, leptin resistance, and finally also to IR and hyperglycemia [19]. Moreover, in several mouse models of AD, including the APP/PS1 mice, the HFD feeding worsened the pathological parameters of AD.

Even though the exact mechanisms responsible for AD progression induced by HFD is not fully understood, there is a possible implication of neuronal IR, and neuroinflammation, but further research must be done [20].

Currently there is no sufficient cure for AD on the market available. However, recently discovered link between obesity, T2DM and AD development revealed new possible strategy for the treatment of neurodegenerative disorders using anorexigenic and/or antidiabetic compounds. One of such compound is prolactin-releasing peptide (PrRP).

PrRP is a neuropeptide that attenuates food intake and increases energy expenditure [21]; nevertheless, because of its peptidic structure, it is not able to cross the blood-brain barrier and act centrally after acute peripheral administration. Our group designed and synthesized several lipidized PrRP analogs increasing the stability of the peptide and allowing it to exert its central anorexigenic and antidiabetic effects after peripheral administration [22].

In our previous studies, we tested the potential neuroprotective properties of palmitoylated PrRP analogs in different mouse models of AD-like pathology and *in vitro*. Palm^{11}-PrRP31 (Figure 1) attenuated hypothermia-induced Tau phosphorylation in the SH-SY5Y cell line and in rat primary cortical neurons [23]. Furthermore, palm^{1}-PrRP31, an analog palmitoylated at the N-terminus, ameliorated hippocampal insulin signaling pathways and attenuated Tau hyperphosphorylation at several epitopes in mice with monosodium glutamate (MSG)-induced obesity [24]. Palm^{11}-PrRP31 also attenuated Tau hyperphosphorylation, improved short-term spatial memory and enhanced synaptic plasticity in transgenic THY-Tau22 mice, a mouse model of tauopathy [25]. Finally, palm^{11}-PrRP31 was shown to significantly reduce amyloid plaque deposition, neuroinflammation and Tau phosphorylation in hippocampi and cortices of APP/PS1 mice [26].

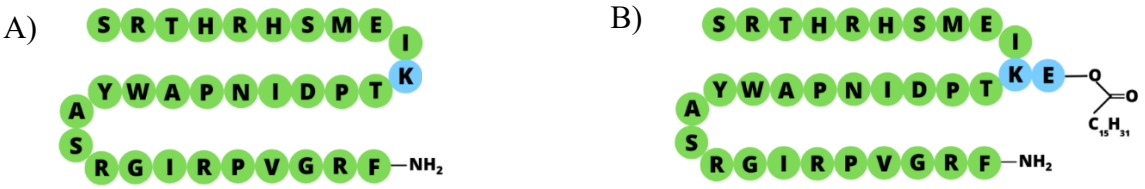

Figure 1: PrRP structures. PrRP31 (A) and its analog (B) palmitoylated through the γ-Glu-linker at Lys^{11} (instead of natural Arg^{11}, palm^{11}-PrRP31).

2. AIMS OF THE THESIS

- **Anti-apoptotic effect of PrRP and its palmitoylated analog palm^{11}-PrRP31 in SH-SY5Y cells**

In the first study, we assessed the effects of PrRP and its palmitoylated analog palm^{11}-PrRP31 in the prevention and after exposure to neurotoxic effect of MG, regarding cell viability and activation of pro- and anti-apoptotic enzymes, in human neuroblastoma cell line SH-SY5Y and rat primary cortical neurons.

- **Effect of palmitoylated PrRP analog on Aβ pathology and microgliosis in APP/PS1 mice**

In the second study, we aimed at the impact of the palm^{11}-PrRP31 treatment on pathological markers associated with AD: Aβ plaques, neuroinflammation, loss of synapses and in the hippocampus, cortex and in the cerebellum in APP/PS1 mouse model of AD pathology.

- **Impact of HFD on metabolic parametres and AD-related pathology in APP/PS1 and WT mice**

In the third part of the thesis, we aimed to find out a potential relationship between insulin resistance and AD-like pathology in the brain and periphery of APP/PS1 mice fed with HFD, a model connecting obesity and AD-like pathology. We assessed the effect of HFD on the Aβ and Tau pathology in the brains and on the central and peripheral inflammation. Furthermore, effect of HFD on the development of substantial peripheral insulin resistance leading to central insulin resistance was determined.

3. METHODS

Human prolactin-releasing peptide (**PrRP31**) (SRTHRHSMEI**R**[11]TPDINPAWYASRGIRPV GRF-NH2) and its lipidized analog palmitoylated in position 11 (**palm[11]-PrRP31**) (SRTHRHSMEI**K**[11] (-E (N-palm))TPDINPAWYASRGIRPVGRF-NH2) were synthesized at the Institute of Organic Chemistry and Biochemistry as previously described [22b].

Anti-apoptotic effect of PrRP and palm[11]-PrRP31 in the prevention and after exposure to toxic MG were studied by *in vitro* studies using **SH-SY5Y** neuroblastoma cell line and **primary rat cortical neurons**. First, the cells were pretreated for 4 h with 1 x 10^{-5} M PrRP31 or palm[11]-PrRP31, or distilled water (blank) to prevent **MG** effects; then, MG was added to a final concentration of 0.6 mM for 16 h. Second, cells were first incubated for 16 h with MG at a final concentration of 0.6 mM and subsequently treated with PrRP31 or palm[11]-PrRP31 at a concentration of 1 x 10^{-5} M for 4 h. Viability was measured by the **MTT test** (3-[4,5-dimethylthiazol-2-yl]-2,5-diphenyl tetrazolium bromide; thiazolyl blue) and activation of apoptotic pathways was measured by western blot (**WB)** as described previously [27].

For the *in vivo* effect of palm[11]-PrRP31 on Aβ pathology and microgliosis, **APP/PS1** mice were used. Male APP/PS1 mice wild-type (WT) controls were fed with Ssniff® R/M-H diet (STD). At the age of 7 months. APP/PS1 mice were twice daily subcutaneously (s.c.) injected with saline (APP/PS1 saline) or **palm[11]-PrRP31** (APP/PS1 palm[11]-PrRP31) at a dose of 5 mg/kg of body weight for 2 months (n = 9-10). WT control group was s.c. injected with saline (control saline). At the end of the experiment, the brains were dissected, stored and used for **WB** and immunohistochemistry (**IHC**) as described previously [28].

APP/PS1 and **WT** mice at the age of 3, 6 and 10 months were used to study the impact of **HFD** on metabolic and neurodegenerative changes. At the age of 2 months, mice were randomly divided into groups of 5 (mice on STD), or 8 (mice on HFD) animals and fed with appropriate diet. At the end of the experiment, the mice were overnight fasted, weighed and plasma samples were collected for determination of the biochemical parameters and an oral glucose tolerance test (OGTT) was performed. Tissue samples were dissected and stored in -80°C until use for **WB** or **IHC** as described previously [28-29].

Statistics: Data are presented as the means ± SEM and were analyzed with GraphPad Software (San Diego, CA, USA). Statistical analysis was performed using unpaired t-test or one-way, followed by Dunnett´s multiple comparisons test or two-way ANOVA with Bonferroni´s multiple comparisons test as indicated in Figures legends and $P<0.05$ was considered statistically significant.

The rate of insulin resistance was expressed with a homeostatic model assessment (HOMA-IR) index [30]

4. RESULTS

4.1 Anti-apoptotic effects of PrRP and its lipidized analog palm^{11}-PrRP31 on SH-SY5Y cells

The results obtained in experiments performed in human neuroblastoma SH-SY5Y cells and primary rat cortical neurons presented in the following chapters were published in International Journal of Molecular Sciences (IJMS) [27].

4.1.1 PrRP31 and palm^{11}-PrRP31 increased cell viability in the prevention and after exposure to neurotoxic effect of MG

0.6 mM MG significantly decreased cell viability compared to that of the vehicle-treated cells. Pretreatment with both PrRP31 and palm^{11}-PrRP31 at a concentration 1x10^{-5} M resulted in significantly increased cell viability in both SH-SY5Y cells (Figure 2A) and rat primary neuronal culture, compared to nonpretreated cells (Figure 2B). 4h treatment with PrRP31 and palm^{11}-PrRP31 at a concentration of 1x10-5 M in SH-SY5Y cells resulted in significantly increased cell viability compared to the nontreated cells treated with 0.6 mM MG (Figure 2C).

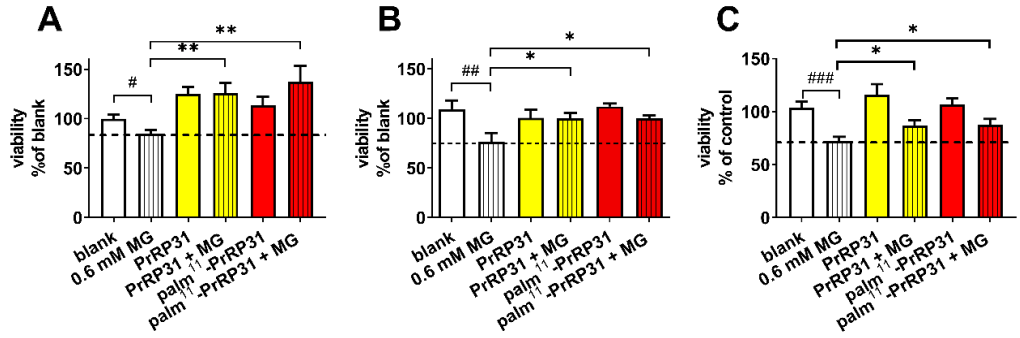

Figure 2. PrRP31 and palm^{11}-PrRP31 significantly increased cell viability during the MG-induced stress. Pretreatment for 4 h with PrRP31 and palm^{11}-PrRP31 at a concentration of: 1x10^{-5} M in SH-SY5Y cells (A), or in rat primary neuronal culture (B), followed by exposure to 0.6 mM MG for 16 h. Treatment for 4 h with PrRP31 and palm^{11}-PrRP31 at a concentration of 1x10^{-5} M, after exposure to 0.6 mM MG for 16 h in SH-SY5Y cells (C). MG toxicity was measured with MTT assay. Data are presented as the means ± SEM as a percentage of blank cells treated with vehicle analysed by Student´s t-test vs 0.6 mM MG #p<0.05, ##p<0.01, ###p<0.001 (dates of sampling n=3, each compound in octuplicates). MG vs treated cells analysed by Student´s t-test, *p<0.05, **p<0,01.

4.1.1.1 PrRP31 and palm^{11}-PrRP31 induced anti-apoptotic signaling in SH-SY5Y cells

As shown in Figure 3, the levels of pro-apoptotic p-Bcl-2-associated death promoter (Bad) (Ser112)/Bad and p-Bad (Ser136)/Bad were increased after MG, and tended to decrease in the cells pretreated with PrRP31 and were significantly decreased in the cells pretreated with palm^{11}-PrRP31. The pro-apoptotic ratio of Bax/Bcl-2 regulators significantly increased after MG exposure was attenuated significantly in the cells pretreated with palm^{11}-PrRP31.

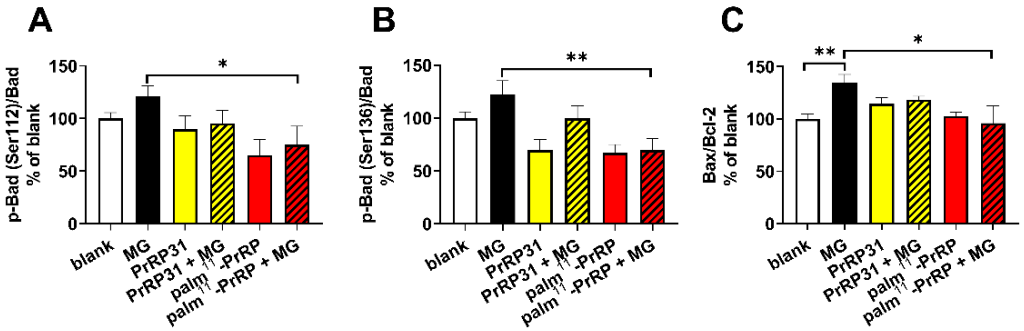

Figure 3. PrRP31 and palm[11]-PrRP31 improved anti-apoptotic signaling in SH-SY5Y cells. Protein levels of p-Bad (Ser112)/Bad (A), p-Bad (Ser136)/Bad (B), Bax/BCl2 (C) were determined by western-blots: SH-SY5Y cells were pretreated with PrRP31 and palm[11]-PrRP31 at a concentration of $1x10^{-5}$ M for 4 h and then stressed with 0.6 mM MG for 16 h. Activation was expressed as the ratio of the activated protein to the total amount of the protein both normalized to loading control, GAPDH. Data are presented as the means ± SEM as a percentage of blank cells treated with medium alone. Analysis is made vs MG by Student´s t-test, *p<0.05, **p<0.01 (each sample in triplicates).

4.2 Effect of palm[11]-PrRP31 analog on pathological markers connected to AD in APP/PS1 mice on standard diet

Results obtained in experiments performed with APP/PS1 mouse model presented in the following chapters were published in Current Alzheimer Research (CAR) [28]. Results confirm and extend previous study from our laboratory [31].

4.2.1 Palm[11]-PrRP31 reduced the Aβ plaque load and microgliosis in the cerebella of APP/PS1 mice

To further study the effects of palm[11]-PrRP31 in APP/PS1 mice, we performed immunohistochemical staining of the cerebellum to assess Aβ plaque load, microgliosis and astrocytosis. Widespread Aβ plaques were found in the cerebella of APP/PS1 mice (Figure 4A), whereas plaques did not develop in the cerebella of control mice (Figure 4C). The number of Aβ plaques was significantly reduced after two months of treatment with palm[11]-PrRP31 (Figure 4B).

Immunohistochemical staining of Iba1, a marker specifically expressed by both resting and activated microglia and macrophages, revealed visible clusters of activated microglia in the cerebella of APP/PS1 mice (Figure 4E). The percentage of the area stained with Iba1 was significantly increased in the APP/PS1 mice compared to their controls, where only resting microglia were visible (Figure 4G). Treatment with palm[11]-PrRP31 (Figure 4F) significantly reduced cerebellar microgliosis.

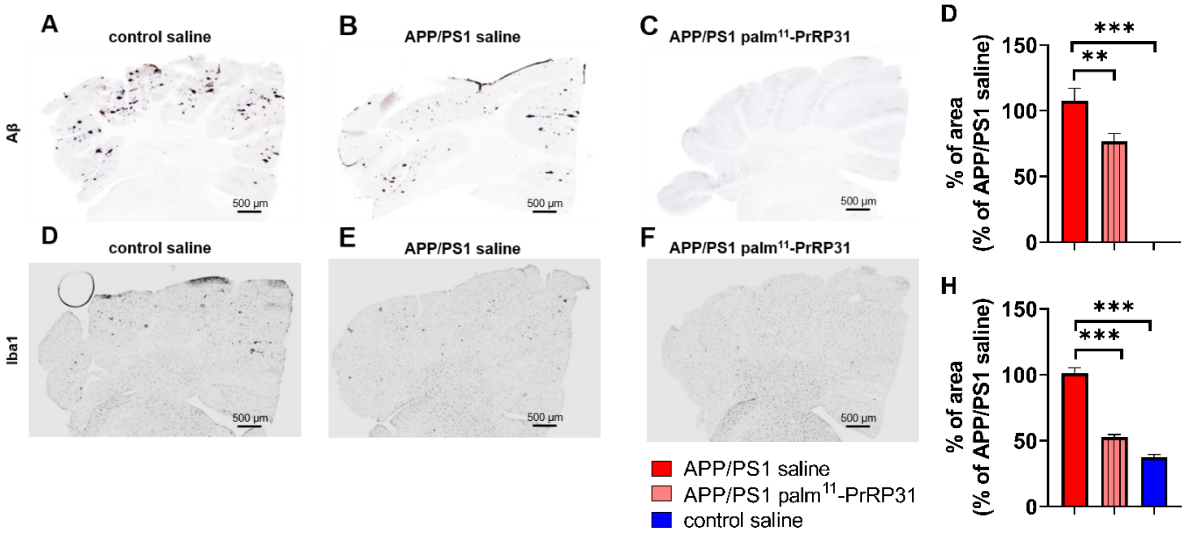

Figure 4: Reduction of β-amyloid plaque load and microgliosis in the cerebellum of the APP/PS1 mice after treatment with palm^{11}-PrRP31. Representative photomicrographs of the saline and palm^{11}-PrRP31 treated APP/PS1 mice and their age-matched controls immunohistochemically stained for human Aβ (A-C) and for microglial marker Iba1 (E-G). Quantification of immunohistochemical staining of human Aβ (D) and microglial marker Iba1 (H) in cerebellum. The data are presented as the means ± SEM. Statistical analysis is made between groups as shown in the graphs by one-way ANOVA with Dunnett post-hoc test, **p<0.01, ***p<0.001 (n = 9-10 mice per group).

4.2.2 Palm^{11}-PrRP31 reduced neuroinflammation in the hippocampi of APP/PS1 mice

We observed increased protein levels of neuroinflammation markers in the hippocampi of APP/PS1 mice, as shown in Figure 5. APP/PS1 mice had slightly increased CD68 (Figure 5A) and significantly increased pro-inflammatory IFNγ (Figure 5B), a commonly used marker of inflammation. Treatment with palm^{11}-PrRP31 significantly decreased both CD68 and IFNγ.

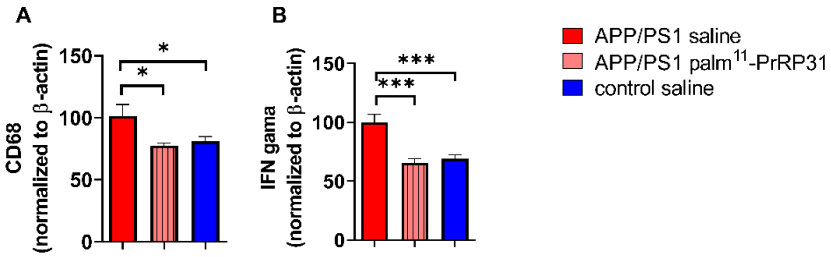

Figure 5: Decreased level of pro-inflammatory proteins in the hippocampi of the APP/PS1 mice after treatment with palm^{11}-PrRP31. Quantification of protein levels of CD68 (A) and IFNγ (B) were determined by WB (n = 8 mice per group). The data are presented as the means ± SEM. Statistical analysis is made between groups as shown in the graphs by one-way ANOVA with Dunnett post-hoc test, *p<0.05, **p<0.01, ***p<0.001.

4.2.3 Palm^{11}-PrRP31 increased synaptogenesis in APP/PS1 mice

IHC revealed a decrease in the postsynaptic marker spinophilin in the hippocampus (Figure 6A) and in the cortex (Figure 6B) of APP/PS1 mice compared to age-matched control mice, which

was reversed by 2 months of treatment with palm[11]-PrRP31, non-significantly in hippocampus and significantly in cortex.

Compared to age-matched control mice, APP/PS1 mice showed significantly reduced protein levels of the postsynaptic marker PSD95 (Figure 6C) and the presynaptic marker syntaxin1A (Figure 6D), measured by WB. After two months of treatment, the protein levels of PSD95 and syntaxin1A were significantly increased in the palm[11]-PrRP31-treated group compared to the APP/PS1 saline-treated group.

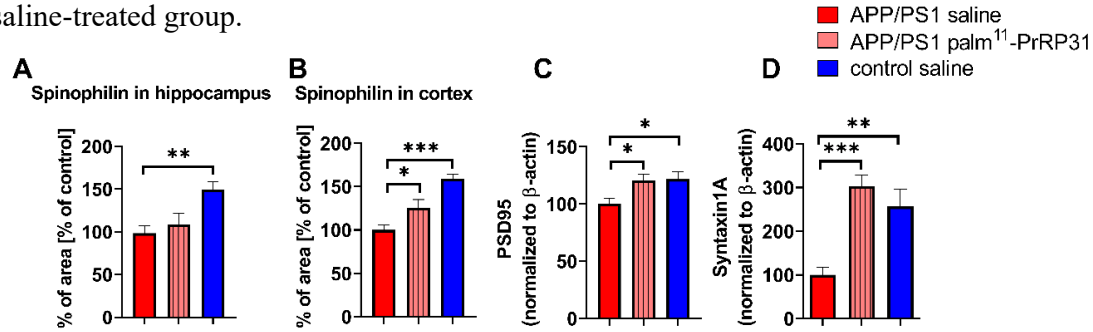

Figure 6: Increase in synaptogenesis in the brains of the APP/PS1 mice after treatment with palm[11]-PrRP31. Quantification of immunohistochemically stained postsynaptic marker spinophilin in hippocampus (A) and cortex (B) and quantification of protein levels of postsynaptic marker PSD95 (C) and presynaptic markers syntaxin1A (D) determined by WB. The data are presented as the means ± SEM. Statistical analysis is made between groups as shown in the graphs by one-way ANOVA with Dunnett post-hoc test, *p<0.05, **p<0.01, ***p<0.001 (n = 5-8 mice per group).

4.2.4 Palm[11]-PrRP31 improved the glymphatic system in the cortex of APP/PS1 mice

Compared to control saline mice, APP/PS1 mice exhibited a nonsignificant decrease in the number of astroglial water channel AQ4, a marker of Aβ clearance, in the hippocampus (Figure 7A)

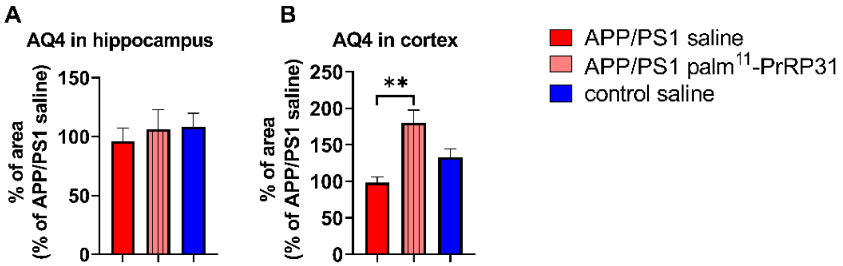

Figure 7: Improvement in glymphatic system in the cortices of the APP/PS1 mice after treatment with palm[11]-PrRP31. Quantification of immunohistochemical staining in the hippocampus (A) and cortex (B) of the saline and palm[11]-PrRP31 treated APP/PS1 mice and their age-matched controls, stained for marker of paravascular glymphatic pathway Aquaporin 4. The data are presented as the means ± SEM. Statistical analysis is made between groups as shown in the graphs by one-way ANOVA with Dunnett post-hoc test, **p<0.01 (n = 5 mice per group).

and a significantly decreased number of AQ4 in the cortex (Figure 7B). Two months of treatment with palm[11]-PrRP31 tended to increase its number in the hippocampus and significantly increased the number of this water channel in the cortex.

4.3 Impact of HFD on metabolic parameters and neurodegeneration in APP/PS1 and WT mice

4.3.1 Effect of HFD on BW, insulin resistance and peripheral inflammation

APP/PS1 and WT mice fed with HFD developed severe obesity, compared to their age-matched controls on STD manifested by significantly increased BW in 6 and 10 months old both APP/PS1 mice and WT mice. Moreover, the BW of 10-month-old. APP/PS1 male mice on HFD was significantly higher than that of their respective age-matched WT controls on HFD (Figure 8A).

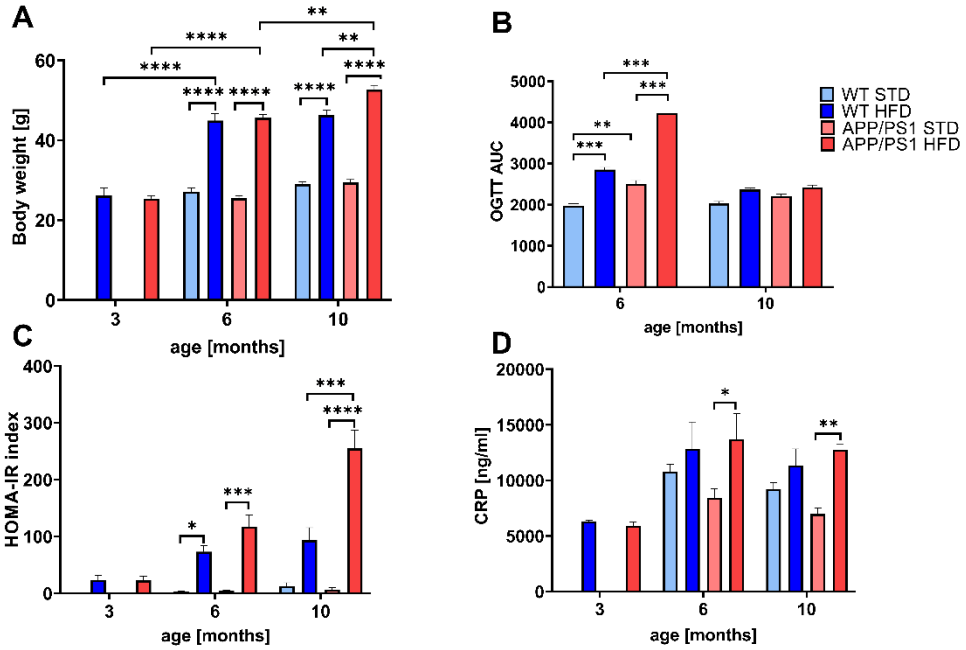

Figure 8: HFD significantly increased BW, HOMA-IR index and CRP. Body weights (A), OGTT after orally administered glucose at a dose 2g/kg (B), HOMA-IR (C) and CRP in fasted plasma (D) in the APP/PS1 mice and their age-matched controls on STD or HFD in 3, 6, or 10 months of age. The data are presented as the means ± SEM. Statistical analysis is made between groups as shown in the graphs by one-way ANOVA with Bonferroni post-hoc test. Significance is *p<0.05, **p<0.01, ***p<0.001, ****p<0.0001 (n = 5-8 mice per group).

In 6 and 10 months, OGTT was performed. The HFD significantly increased area under curve (AUC) in 6 months in both strains, suggesting glucose intolerance of the mice (Figure 8B). In addition, APP/PS1 mice on HFD showed significantly increased glucose intolerance in comparison with WT mice of the same age on HFD and APP/PS1 on STD showed significant increase in glucose level in comparison with WT mice on STD. However, at 10 months of age, no difference was obvious among the groups.

All mice fed with HFD showed a significantly higher HOMA-IR index than their age- and genotype-matched STD-fed mice (Figure 8C), which indicates increased peripheral IR. HOMA-IR of 10 months-old APP/PS1 mice on HFD was also significantly increased in comparison with their age-matched WT controls on HFD. The HFD-induced obesity led to a significant increase of CRP,

marker of peripheral inflammation, in the fasted plasma of APP/PS1 mice in 6 and 10 months of age (Figure 8D) in comparison with their age-matched controls on STD.

4.3.2 HFD caused liver steatosis

HFD feeding caused a significant increase in liver weight in 6- and 10-month-old APP/PS1 mice, while it only tended to increase the liver weight of WT mice as shown in Figure 8A. Furthermore, livers of 10-month-old APP/PS1 mice on HFD were significantly heavier than those of their respective WT controls on HFD (Figure 9A). Increase in liver weight was mainly caused by abnormal retention of fat within the livers, an obvious liver steatosis. Mice in 3 months of age did not develop any signs of steatosis and no significant difference was found between the strains. In 6 and 10 months of age, both APP/PS1 and WT mice on HFD developed steatosis. However, only in APP/PS1 mice fed HFD the increase in steatosis was statistically significant. Furthermore, APP/PS1 mice on HFD developed significant gain in steatosis in 6 months in comparison to WT on HFD shown in Figure 9B. STD-fed mice did not show any evidence of liver steatosis, even at a late age.

Level of fibrosis was measured only in 6- and 10-months old mice, after they developed the steatosis. APP/PS1 and WT mice on HFD developed mild fibrosis already in 6 months of age, compared to their age-matched controls on STD that was significantly pronounced in both strains in 10 months of age as shown in the Figure 9C.

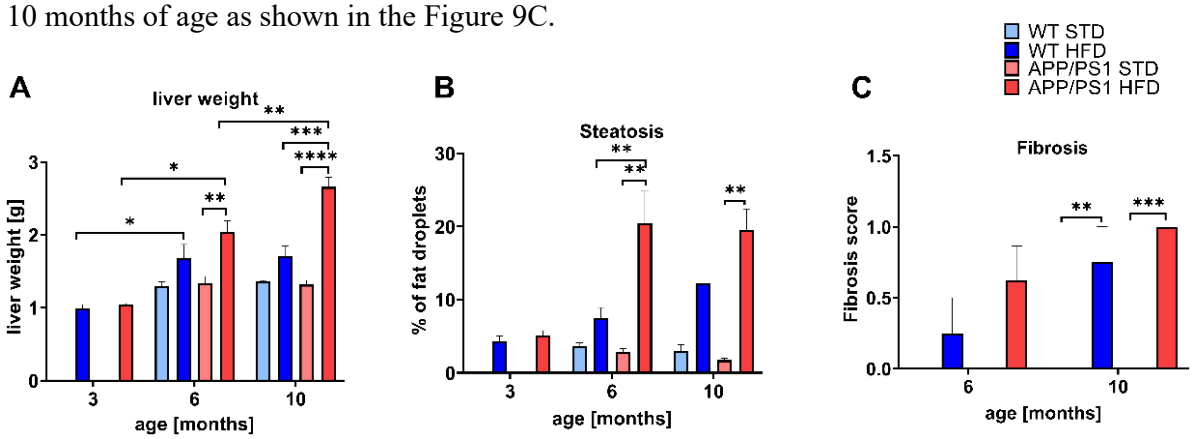

Figure 9: HFD caused hepatomegaly, liver steatosis and fibrosis. Quantification of liver weights (A) and livers stained by hematoxylin-eosin for steatosis (B) and by the fibrotic liver staining (C). The data are presented as the means ± SEM. Statistical analysis is made between groups as shown in the graphs by one-way ANOVA with Bonferroni post-hoc test. Significance is *p<0.05, **p<0.01, ***p<0.001, ****p<0.0001 (n = 5-8 mice per group).

4.3.3 Effects of HFD on the development of AD-like pathology

4.3.3.1 HFD exacerbated the Aβ plaque load in the hippocampi and cortices of APP/PS1 mice

Photomicrographs of immunohistochemically stained brain sections showed the development of extensive Aβ plaque loads both in the hippocampi and cortices of APP/PS1 mice (Figure 10), starting in 3 months and developing with age. Whereas control mice (Figure 10A) did not develop

any plaques. HFD significantly exacerbated the Aβ plaque loads in cortices of 10-month-old APP/PS1 mice as shown in Figure 10F, compared to APP/PS1 mice on STD (10C).

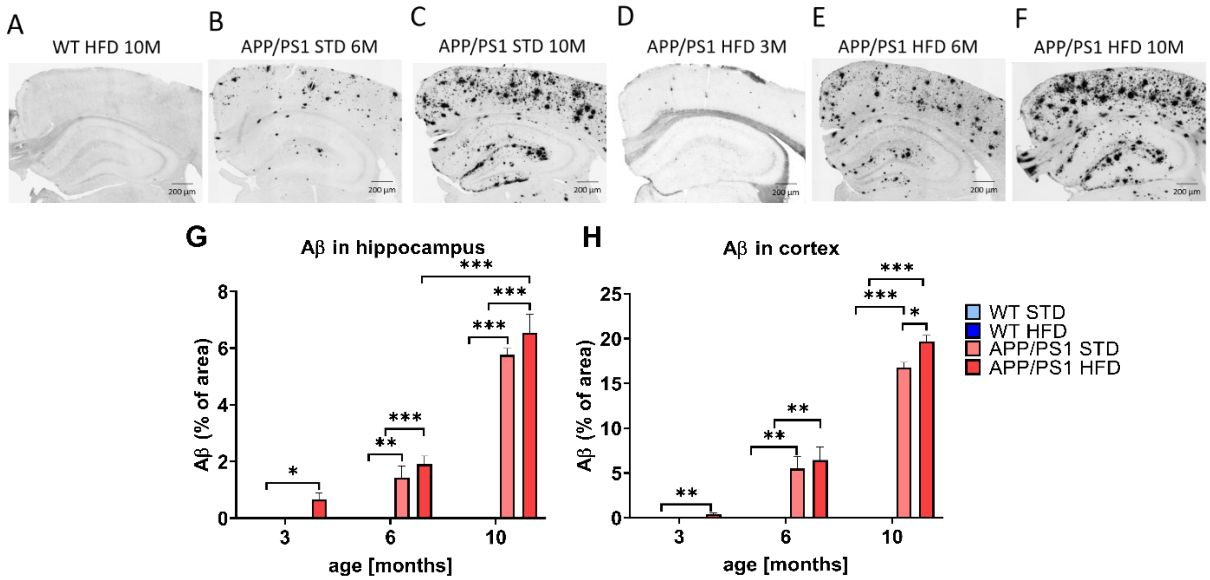

Figure 10: HFD exacerbated Aβ plaque load in the cortices of 10-month-old APP/PS1 mice. Representative photomicrographs of the APP/PS1 mice fed either with STD in 6 months (B) 10 months (C), or HFD in 3 months (D) 6 months (E) and 10 months (F) of age and the WT control in 10 months of age (A) immunohistochemically stained (A-F) for human Aβ and their quantification (G, H). Aβ plaque load is expressed as a percentage of the stained area. The data are presented as the means ± SEM. Statistical analysis is made between groups as shown in the graphs by one-way ANOVA with Bonferroni post-hoc test, *p<0.05, **p<0.01, ***p<0.001 (n = 5-8 mice per group).

4.3.3.2 HFD worsened neuroinflammation in the brains of APP/PS1 mice

Immunohistochemical microglial staining of Iba1 revealed visible clusters of activated microglia in the hippocampi and cortices of APP/PS1 mice on STD of both ages (Figure 11) but not

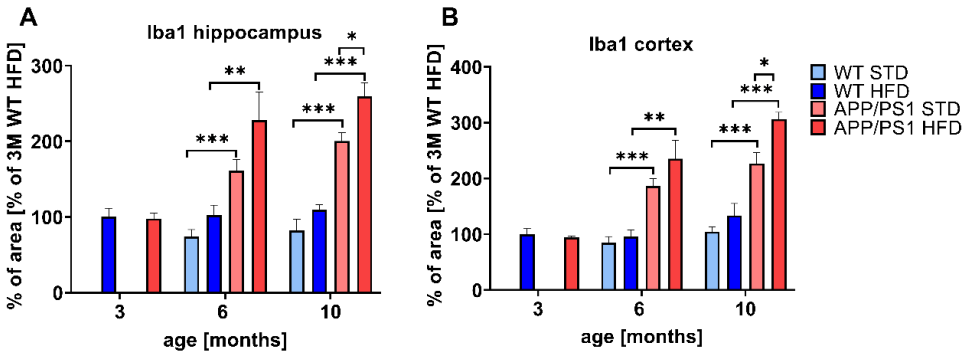

Figure 11: Effect of HFD on microgliosis in the hippocampi and cortices of the APP/PS1 mice. Quantification of the microgliosis determined by IHC in both, hippocampus (A) and cortex (B) of APP/PS1 and WT mice fed either with STD, or HFD. Percentage of the stained area is expressed as a % of the 3-month-old WT mice on HFD to enable the comparison of multiple staining series. The data are presented as the means ± SEM. Statistical analysis is made between groups as shown in the graphs by one-way ANOVA with Bonferroni post-hoc test, *p<0.05, **p<0.01, ***p<0.001 (n = 5-8 mice per group).

in the brains of WT control mice, where only resting microglia were visible. HFD significantly increased level of microgliosis in both hippocampi and cortices of 10-month-old APP/PS1 mice compared to APP/PS1 on STD as shown in Figure 11.

4.3.3.3 Increased Tau phosphorylation in the hippocampi and cortices of APP/PS1 mice

Immunohistochemical staining revealed increased number of phosphorylated Tau at Ser202 and Thr205 (AT8 antibody) in dystrophic neurites in hippocampi and cortices of APP/PS1 mice as shown in Figure 12. The Tau phosphorylation is detectable already in 3 months and increases with the age and spreading of Aβ pathology. HFD significantly increased number of AT8 clusters formed around the Aβ plaques in the cortices and hippocampi of 6-month-old APP/PS1 mice. HFD also significantly increased size of the AT8 clusters in the hippocampi and cortices of 6-month-old APP/PS1 mice (Figure 12).

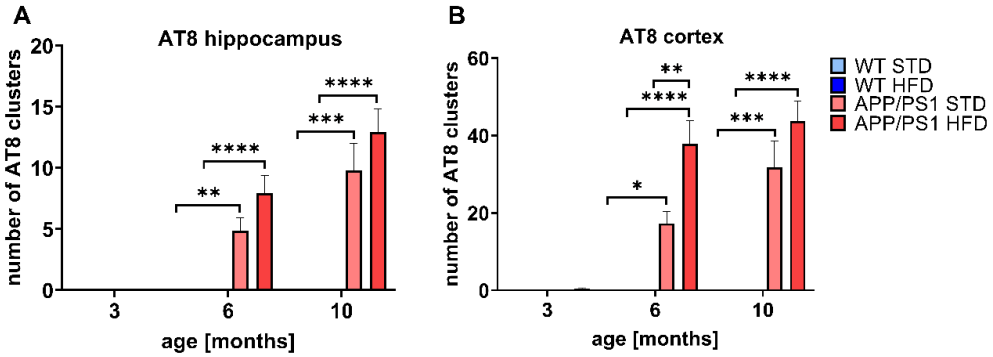

Figure 12: Increased Tau phosphorylation around Aβ plaques in hippocampi and cortices of APP/PS1 mice. Quantification of the AT8 antibody recognizing p-Tau at Ser202 and Thr205 in both, hippocampus (A) and cortex (B) of APP/PS1 and WT mice fed either with STD, or HFD determined by IHC. The data are presented as the means ± SEM. Statistical analysis is made between groups as shown in the graphs by one-way ANOVA with Bonferroni post-hoc test, *p<0.05, **p<0.01, ***p<0.001, ****p<0.0001 (n = 5-8 mice per group).

4.3.3.4 HFD and age attenuated the PI3K/Akt signaling pathway in the hippocampus

Level of IRβ significantly increased in time in hippocampi of WT and APP/PS1 mice, however, HFD reversed this effect; significantly decreased IRβ was observed in the hippocampus of 10-month-old APP/PS1 on HFD compared to APP/PS1 mice on STD (Figure 13D). Furthermore, levels of PI3K p85 also significantly decreased in 10-month-old APP/PS1 mice on HFD compared to their age-matched controls on STD, but also compared to 10-month-old WT mice on HFD. No differences were observed in levels of Akt, nevertheless, its phosphorylation at Ser473 tended to decrease with HFD at 6 months old WT and AP/PS1 mice, and significantly decreased between 6th and 10th month of age, as indicated in Figure 13G.

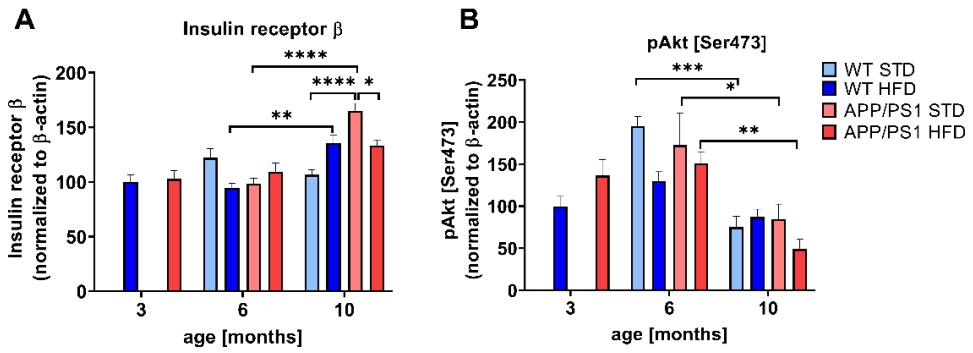

Figure 13: HFD and age attenuated the PI3K/Akt signaling pathway in the hippocampus. Quantification of protein levels of (A) Insulin receptor β and (B) p-Akt (Ser473), determined by WB. Statistical analysis is made between groups as shown in the graphs by one-way ANOVA with Bonferroni post-hoc test, *p<0.05, **p<0.01, ***p<0.001, and ****p<0.0001 (n = 5 mice per group).

5. DISCUSSION

Obesity and related IR have been established as risk factors for the development of AD, resulting in intensive research of metabolic and pathological changes, which are caused by both diseases in the CNS [10b]. Currently, there is no sufficient AD treatment because the exact mechanisms leading to AD progression are still not fully elucidated. However, increasing evidence show that anorexigenic and antidiabetic peptides could be potential powerful neuroprotective agents, but their mechanism of action is poorly understood.

In my PhD thesis, potential neuroprotective effects of anorexigenic neuropeptide PrRP31 and its lipidized analog palm^{11}-PrRP31 were studied *in vitro*, namely in MG affected neuroblastoma SH-SY5Y cells and rat primary cortical neurons and *in vivo* in APP/PS1 mouse transgenic model of AD. Furthermore, we examined a possible relationship among diet-induced obesity, IR, and inflammation in the periphery and development of neuropathological changes in the brain of WT or APP/PS1 mice fed with HFD.

We investigated effect of PrRP31 and palm^{11}-PrRP31 in SH-SY5Y cells and rat primary cortical neurons affected by neurotoxic MG that is correlated with an increase in oxidative stress in AD [32] and it is a useful tool for screening of potential neuroprotective compounds that could ameliorate oxidative stress [33]. PrRP31 and palm^{11}-PrRP31 increased SH-SY5Y cell viability determined by the MTT test in the MG-stressed SH-SY5Y cells. Furthermore, pretreatment of SH-SY5Y and primary cortical neurons with both PrRP31 and palm^{11}-PrRP31 significantly enhanced viability of the cells affected with MG. Moreover, both PrRP31 and palm^{11}-PrRP31

attenuated level of pro-apoptotic enzymes and increased level of prosurvival proteins in the MG-stressed cells [27].

Chronic effects of palm^{11}-PrRP31 analog on pathological markers connected to AD were studied in the hippocampus, cortex and cerebellum of APP/PS1 mice on standard diet. We confirmed significant reduction of the number of Aβ plaques and level of inflammation not only in the hippocampi and cortices, but also in the cerebella of APP/PS1 mice after palm^{11}-PrRP31 treatment. Neuroprotective effect of palm^{11}-PrRP31 was also proved by increased synaptogenesis in the hippocampi of APP/PS1 mice and by increased number of the astrocytic water channels AQ4 pointing to improved Aβ peptide clearance via the glymphatic pathway [28].

To assess the effect obesity resulting in peripheral IR and inflammation on AD progression, WT and APP/PS1 mice were fed either with HFD or STD from 2 months of age and followed at 3, 6 and 10 months. As expected, chronic intake of HFD significantly increased body weight, peripheral and hippocampal insulin resistance and induced obesity and prediabetes in the mice [34]. Beyond, mice on HFD developed hepatomegaly, steatosis and fibrosis. Interestingly, APP/PS1 on HFD mice further developed significant increase in all mentioned parameters compared to WT mice. Moreover, APP/PS1 mice on HFD developed significant increase in chronic peripheral inflammation. These results suggest AD-related pathology interacts with HFD in aggravating the parameters connected to obesity and insulin resistance in the mice.

Pathological markers connected to AD, such as Aβ and Tau pathology, and microgliosis were all exacerbated in the hippocampus and cortex of APP/PS1 mice fed with HFD. Furthermore, in our study, strong correlation was found between peripheral (CRP) and central (Iba1) inflammation that was calculated in the whole set of mice (Pearson r: 0.3028, p=0.0198), giving a strong evidence suggesting that inflammation is one of the main denominators of obesity and AD [35].

Moreover, HFD decreased insulin signaling in the hippocampus of the mice, suggesting development of central IR. In our study, strong negative correlations were computed between peripheral IR (HOMA-IR index) and hippocampal level of PI3K (Pearson r: -0.3226, p=0.0253) and p-Akt (Ser473) (Pearson r: -0.2941, p=0.0448) as markers of central IR. These data show that hyperinsulinemia, which can be induced by obesity, could lead to reduced activation of insulin signaling in the brain and prove strong evidence of IR being an interconnection between obesity, and AD-like pathology development.

6. CONCLUSIONS

Neuroprotective effects of anorexigenic neuropeptide PrRP and its palmitoylated analog palm^{11}-PrRP31 were proved *in vitro* using MG induced cytotoxicity in SH-SY5Y cells and rat primary cortical neurons and *in vivo* in APP/PS1 mice, a transgenic model of AD.

Firstly, in *in vitro* study, PrRP and palm^{11}-PrRP31 increased viability in the MG-stressed SH-SY5Y cells and primary cortical cells by prevention of the apoptosis in the cells, which could be one of the potential mechanisms implicated in the neuroprotective properties of PrRP.

In the following *in vivo* studies, palm^{11}-PrRP31 exhibited multiple beneficial neuroprotective effects in APP/PS1 mice, a mouse model of AD-like Aβ pathology. Palm^{11}-PrRP31 significantly reduced the Aβ plaque load by improved clearance via glymphatic pathway and attenuated microgliosis not only in the hippocampi and cortices, but also in the cerebella of APP/PS1 mice. Treatment with palm^{11}-PrRP31 also supported synaptogenesis.

Based on the results from the two studies, we would like to conclude that PrRP is a promising agent for alleviating different changes that occur in neurodegenerative disorders and it might be a potential drug against neurodegenerative disorders including Alzheimer´s disease.

To conclude our study of possible relationship among diet-induced obesity, IR, and inflammation in the periphery and development of neuropathological changes in the brain, HFD-related obesity worsened metabolic parameters connected to obesity, leading to glucose intolerance, insulin resistance and chronic peripheral inflammation. These dysregulations further promote disturbances in hippocampal insulin signaling and neuroinflammation, leading to a worsening of Aβ and Tau pathology in APP/PS1 mice. Moreover, mice on HFD developed significant increase in liver weight and its abnormality, such as liver steatosis, or fibrosis.

Furthermore, we found a strong correlation not only between the peripheral and central insulin resistance, but also between the peripheral and central inflammation, both in APP/PS1 and WT mice. These results support the theory of inflammation and insulin resistance being the main common factors between obesity and AD.

7. REFERENCES

[1] S. Duong, T. Patel, F. Chang, *Can Pharm J (Ott)* **2017**, *150*, 118-129.

[2] aG. S. Bloom, *JAMA Neurol* **2014**, *71*, 505-508; bA. Serrano-Pozo, M. L. Mielke, T. Gomez-Isla, R. A. Betensky, J. H. Growdon, M. P. Frosch, B. T. Hyman, *Am J Pathol* **2011**, *179*, 1373-1384.

[3] aM. T. Heneka, M. K. O'Banion, *J Neuroimmunol* **2007**, *184*, 69-91; bM. Fakhoury, *Curr Neuropharmacol* **2018**, *16*, 508-518.

[4] M. T. Heneka, M. J. Carson, J. El Khoury, G. E. Landreth, F. Brosseron, D. L. Feinstein, A. H. Jacobs, T. Wyss-Coray, J. Vitorica, R. M. Ransohoff, K. Herrup, S. A. Frautschy, B. Finsen, G. C. Brown, A. Verkhratsky, K. Yamanaka, J. Koistinaho, E. Latz, A. Halle, G. C. Petzold, T. Town, D. Morgan, M. L. Shinohara, V. H. Perry, C. Holmes, N. G. Bazan, D. J. Brooks, S. Hunot, B. Joseph, N. Deigendesch, O. Garaschuk, E. Boddeke, C. A. Dinarello, J. C. Breitner, G. M. Cole, D. T. Golenbock, M. P. Kummer, *Lancet Neurol* **2015**, *14*, 388-405.

[5] J. J. Iliff, M. Wang, Y. Liao, B. A. Plogg, W. Peng, G. A. Gundersen, H. Benveniste, G. E. Vates, R. Deane, S. A. Goldman, E. A. Nagelhus, M. Nedergaard, *Science Translational Medicine* **2012**, *4*, 147ra111.

[6] C. R. Jack, Jr., D. S. Knopman, W. J. Jagust, L. M. Shaw, P. S. Aisen, M. W. Weiner, R. C. Petersen, J. Q. Trojanowski, *Lancet Neurol* **2010**, *9*, 119-128.

[7] S. Hong, V. F. Beja-Glasser, B. M. Nfonoyim, A. Frouin, S. Li, S. Ramakrishnan, K. M. Merry, Q. Shi, A. Rosenthal, B. A. Barres, C. A. Lemere, D. J. Selkoe, B. Stevens, *Science* **2016**, *352*, 712-716.

[8] aM. C. Miniaci, E. De Leonibus, *F1000Res* **2018**, *7*, 168; bE. Hoxha, P. Lippiello, F. Zurlo, I. Balbo, R. Santamaria, F. Tempia, M. C. Miniaci, *Front Aging Neurosci* **2018**, *10*, 396.

[9] aC. L. Joachim, J. H. Morris, D. J. Selkoe, *Am J Pathol* **1989**, *135*, 309-319; bM. K. Singh-Bains, V. Linke, M. D. R. Austria, A. Y. S. Tan, E. L. Scotter, N. F. Mehrabi, R. L. M. Faull, M. Dragunow, *Neurobiol Dis* **2019**, *132*, 104589.

[10] aL. Plum, M. Schubert, J. C. Brüning, *Trends Endocrinol Metab* **2005**, *16*, 59-65; bS. Tabassum, A. Misrani, L. Yang, *Front Hum Neurosci* **2020**, *14*, 602360-602360.

[11] S. H. Kim, G. M. Reaven, *Diabetes Care* **2008**, *31*, 1433-1438.

[12] Z. Berger, H. Roder, A. Hanna, A. Carlson, V. Rangachari, M. Yue, Z. Wszolek, K. Ashe, J. Knight, D. Dickson, C. Andorfer, T. L. Rosenberry, J. Lewis, M. Hutton, C. Janus, *J Neurosci* **2007**, *27*, 3650-3662.

[13] J. Sripetchwandee, N. Chattipakorn, S. C. Chattipakorn, *Front Endocrinol (Lausanne)* **2018**, *9*, 496.

[14] S. M. de la Monte, J. R. Wands, *J Diabetes Sci Technol* **2008**, *2*, 1101-1113.

[15] F. Amicarelli, S. Colafarina, F. Cattani, A. Cimini, C. Di Ilio, M. P. Ceru, M. Miranda, *Free Radical Biology and Medicine* **2003**, *35*, 856-871.

[16] M. Tajes, A. Eraso-Pichot, F. Rubio-Moscardó, B. Guivernau, M. Bosch-Morató, V. Valls-Comamala, F. J. Muñoz, *Neuroscience Letters* **2014**, *580*, 78-82.

[17] aL. A. Hulshof, L. A. Frajmund, D. van Nuijs, D. C. N. van der Heijden, J. Middeldorp, E. M. Hol, *Neurobiology of Aging* **2022**, *113*, 28-38; bL. Chen, S. Xu, T. Wu, Y. Shao, L. Luo, L. Zhou, S. Ou, H. Tang, W. Huang, K. Guo, J. Xu, *Aging (Albany NY)* **2019**, *11*, 10242-10251.

[18] D. Bagnol, H. A. Al-Shamma, D. Behan, K. Whelan, A. J. Grottick, *Curr Protoc Neurosci* **2012**, *Chapter 9*, Unit 9.38.31-13.

[19] R. Buettner, J. Schölmerich, L. C. Bollheimer, *Obesity (Silver Spring)* **2007**, *15*, 798-808.

[20] aE. M. Knight, I. V. Martins, S. Gümüsgöz, S. M. Allan, C. B. Lawrence, *Neurobiol Aging* **2014**, *35*, 1821-1832; bM. Kacirova, B. Zelezna, M. Blazkova, M. Holubova, A. Popelova, J. Kunes, B. Sediva, L. Maletinska, *J Neuroinflammation* **2021**, *18*, 141; cX. Fan, B. Liu, J. Zhou, X. Gu, Y. Zhou, Y. Yang, F. Guo, X. Wei, H. Wang, N. Si, J. Yang, B. Bian, H. Zhao, *Front Aging Neurosci* **2021**, *13*, 658376.
[21] aM. Bjursell, M. Lennerås, M. Göransson, A. Elmgren, M. Bohlooly-Y, *Biochemical and Biophysical Research Communications* **2007**, *363*, 633-638; bV. Prazienkova, A. Popelova, J. Kunes, L. Maletinska, *Int J Mol Sci* **2019**, *20*.
[22] aL. Maletínská, V. Nagelová, A. Tichá, J. Zemenová, Z. Pirník, M. Holubová, A. Špolcová, B. Mikulášková, M. Blechová, D. Sýkora, Z. Lacinová, M. Haluzík, B. Železná, J. Kuneš, *International Journal Of Obesity* **2015**, *39*, 986; bV. Pražienková, M. Holubová, H. Pelantová, M. Bugáňová, Z. Pirník, B. Mikulášková, A. Popelová, M. Blechová, M. Haluzík, B. Železná, M. Kuzma, J. Kuneš, L. Maletínská, *PLOS ONE* **2017**, *12*, e0183449.
[23] V. Prazienkova, C. Schirmer, M. Holubova, B. Zelezna, J. Kunes, M. C. Galas, L. Maletinska, *J Alzheimers Dis* **2019**, *67*, 1187-1200.
[24] A. Spolcova, B. Mikulaskova, M. Holubova, V. Nagelova, Z. Pirnik, J. Zemenova, M. Haluzik, B. Zelezna, M. C. Galas, L. Maletinska, *J Alzheimers Dis* **2015**, *45*, 823-835.
[25] A. Popelova, V. Prazienkova, B. Neprasova, B. J. Kasperova, L. Hruba, M. Holubova, J. Zemenova, D. Blum, B. Zelezna, M. C. Galas, J. Kunes, L. Maletinska, *J Alzheimers Dis* **2018**, *62*, 1725-1736.
[26] M. Holubova, L. Hruba, A. Popelova, M. Bencze, V. Prazienkova, S. Gengler, H. Kratochvilova, M. Haluzik, B. Zelezna, J. Kunes, C. Holscher, L. Maletinska, *Neuropharmacology* **2019**, *144*, 377-387.
[27] A. Zmeskalova, A. Popelova, A. Exnerova, B. Zelezna, J. Kunes, L. Maletinska, *Int J Mol Sci* **2020**, *21*.
[28] A. Mengr, L. Hrubá, A. Exnerová, M. Holubová, A. Popelová, B. Železná, J. Kuneš, L. Maletínská, *Curr Alzheimer Res* **2021**, *18*, 607-622.
[29] L. Kořínková, M. Holubová, B. Nepraśová, L. Hrubá, V. Strnadová, M. Bencze, M. Haluzik, J. Kunes, L. Maletinska, B. Zelezná, *Journal of Molecular Endocrinology* **2019**, *64*.
[30] M. C. Lansang, G. H. Williams, J. S. Carroll, *American Journal of Hypertension* **2001**, *14*, 51-53.
[31] M. Holubová, L. Hrubá, A. Popelová, M. Bencze, V. Pražienková, S. Gengler, H. Kratochvílová, M. Haluzík, B. Železná, J. Kuneš, C. Hölscher, L. Maletínská, *Neuropharmacology* **2019**, *144*, 377-387.
[32] C. Angeloni, L. Zambonin, S. Hrelia, *Biomed Res Int* **2014**, *2014*, 238485-238485.
[33] J. Bellier, M. J. Nokin, E. Larde, P. Karoyan, O. Peulen, V. Castronovo, A. Bellahcene, *Diabetes Res Clin Pract* **2019**, *148*, 200-211.
[34] L. Mráziková, B. Neprašová, A. Mengr, A. Popelová, V. Strnadová, L. Holá, B. Železná, J. Kuneš, L. Maletínská, *Front Pharmacol* **2021**, *12*, 779962.
[35] M. Kacirova, A. Zmeskalova, L. Korinkova, B. Zelezna, J. Kunes, L. Maletinska, *Clin Sci (Lond)* **2020**, *134*, 547-570.

LIST OF MY PUBLICATIONS

Publications related to Ph.D. thesis:

1. Kacířová M, **Zmeškalová A**, Kořínková L, Železná B, Kuneš J, Maletínská L. Inflammation: major denominator of obesity, Type 2 diabetes and Alzheimer's disease-like pathology? Clin Sci (Lond). 2020 Mar 13; 134(5):547-570. doi: 10.1042/CS20191313. PMID: 32167154. **IF = 6.876**
2. **Zmeškalová A**, Popelová A, Exnerová A, Železná B, Kuneš J, Maletínská L. Cellular Signaling and Anti-Apoptotic Effects of Prolactin-Releasing Peptide and Its Analog on SH-SY5Y Cells. Int. J. Mol. Sci. 2020 Sep 1; *21*(17): 6343. doi: 10.3390/ijms21176343. PMID: 32882929, PMCID: PMC7503370. **IF = 6.208**
3. **Mengr A**, Hrubá L, Exnerová A, Holubová M, Popelová A, Železná B, Kuneš J, Maletínská L. Palmitoylated Prolactin-releasing Peptide Reduced Aβ Plaques and Microgliosis in the Cerebellum: APP/PS1 Mice Study. Curr Alzheimer Res. 2021 Sep 22; 18: 607-622. doi: 10.2174/1567205018666210922110652, PMID: 34551697. **IF = 3.040**
4. Mráziková L, Neprašová B, **Mengr A**, Popelová A, Strnadová V, Holá L, Železná B, Kuneš J, Maletínská L. Lipidized Prolactin-Releasing Peptide as a New Potential Tool to Treat Obesity and Type 2 Diabetes Mellitus: Preclinical Studies in Rodent Models. Front Pharmacol. 2021 Nov 18; 12:779962. doi: 10.3389/fphar.2021.779962. PMID: 34867411; PMCID: PMC8637538. **IF = 5.988**